



# Design of Pt/C X-ray supermirror by needle optimization

Xiaodong Wang<sup>a,\*</sup>, Hai Tian<sup>b</sup>, Shuai Ren<sup>a</sup>, Peng Zhou<sup>a</sup>, Bo Chen<sup>a</sup>

<sup>a</sup> Changchun Institute of Optics, Fine Mechanics and Physics, Chinese Academy of Sciences, Changchun 130033, China

<sup>b</sup> Science and Technology on Vacuum Technology and Physics Laboratory, Lanzhou 730000, China

## ARTICLE INFO

### Keywords:

Needle optimization  
Pt/C  
X-ray  
Supermirror

## ABSTRACT

Needle optimization is widely used in visible and infrared region, but it is rarely utilized in X-ray and extreme ultraviolet waveband. We use Needle optimization to design Pt/C X-ray supermirrors, and the grazing incidence angles are 1.0, 1.4, and 1.7 degree, respectively. A modified target is introduced into optilayer software. A good result is obtained by Optilayer software combined with IMD software. The difference of design results between block method and needle optimization is discussed.

## 1. Introduction

In X-ray and extreme ultraviolet (EUV) region, block method [1], power law method [2], numerical and analytical method [3] are often used to design optical thin film mirrors. In block method, a multilayer mirror is divided into several blocks, and the block is periodic multilayer. Each block can reflect some specific waveband based on Bragg diffraction principle. The advantage of this method is easy to be fabricated, and there is no need for precise control of deposition velocity. Needle optimization method widely used in visible and infrared waveband is rarely utilized in X-ray and EUV region. In this method, a new layer is inserted into existing multilayer, it changes refractive-index profile, and this insertion will improve or deteriorate optical performance [4]. Only Tikhonravov group designed broad angular mirror by needle optimization method in Optilayer software [5,6].

In X-ray, layer thickness in the mirror is about several nanometres. The negative influence of interface roughness and diffusion on specular reflectivity cannot be ignored. The reflectivity reduction due to roughness can be calculated by the Debye–Waller factor,  $\exp(-16\pi^2\sigma_L^2 \cos^2 \theta / \lambda^2)$  [7]. IMD, as a widely used design tool in EUV and X-ray, introduces five kinds of interface profile functions to describe this effect, and they are Error, Exponential, Linear, Sinusoidal, and step functions. Error function shows a better agreement with most of experimental results, and it is a default setting [8]. However, Optilayer, as a successful design software in visible and infrared waveband, utilizes one unknown interlayer profile function to calculate the influence of interlayer on optical performance, and this restricts its application in X ray region.

In X-ray, supermirrors refer to that work in a wide waveband region or broad angular region. Mirrors often work by virtue of total reflection in grazing incidence because of high transmittance for materials [9]. Grazing incidence angle is a key parameter in X-ray optical system. High grazing incidence angle can shorten focus length, enhance

collective area, and reduce cost of optical system. In ATHENA, the mirror works at the grazing incidence angle of up to 1.752 degree in 0.1–10 keV. However, they did not give their reflectance curves [10].

In this paper, we use the gradual evolution version of the needle optimization technique to design supermirrors in 0.2–10 keV, and the grazing incidence angles are 1.0, 1.4, and 1.7, respectively. The design results derived from the needle optimization is compared with that derived from block method.

## 2. Design

In X-ray, Pt/C multilayer was used in Nustar [11] and ASTRO-H [12]. Due to its proved stability in long-term space missions, we also choose Pt/C as material pair. The substrate is fused silica with a surface roughness of 0.45 nm. Interlayer roughness/diffusion is assumed to be 0.45 nm. There are three parts in our design strategy: first, we build a modified target combined with roughness effect; second, we use Needle optimization in Optilayer software to design supermirrors; third, we utilize genetic algorithm in IMD software to do further refinement.

### 2.1. A modified target combined with roughness effect

Fig. 1 shows design results (black line) at 1.7 degree obtained by Optilayer software. Thin film removal, design cleaner, and Interlayer refinement were conducted after the gradual evolution version of the needle optimization. The reflectance target is 10% in 2.5–10 keV at 1.7 degree. It seems that we got a good result. However, we put our thickness distribution into IMD software, and, as shown in Fig. 1, it is found that reflectance curve (red line) get worse if we select Error function in interface profile function in IMD, but result (not shown) shows a good agreement with the one obtained from Optilayer if we

\* Corresponding author.

E-mail address: [wangxiaodong@ciomp.ac.cn](mailto:wangxiaodong@ciomp.ac.cn) (X. Wang).

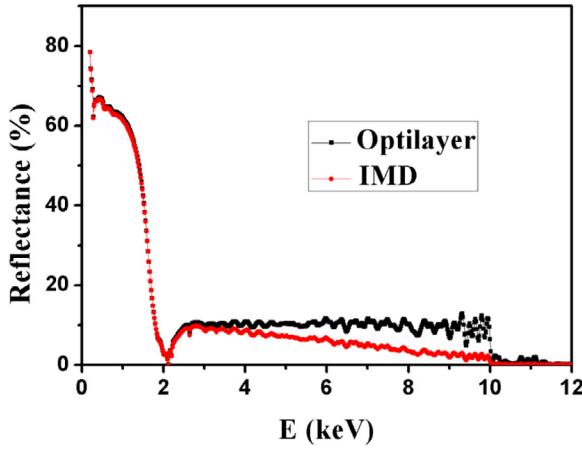


Fig. 1. Design at 1.7 degree obtained by optilayer shows a worse performance in IMD.

select Exponential function in interface profile function in IMD. Thus, a new method, instead of interlayer function in optilayer, must be used to describe negative effect of interface roughness on optical performance of mirrors.

Error function is defined by Eq. (1), and Exponential function is defined by Eq. (2), where  $w$  is derivative of the interface profile,  $s = 4\pi \sin \theta / \lambda$ , and  $\sigma$  is roughness [13]. Error function is more appropriate than Exponential function to describe interface profile of most of materials deposited by magnetron sputtering. Thus, Error function must be introduced into designing by Optilayer software. As shown in Eq. (3), a new target [3] is introduced to replace the old one, where  $\sigma$  is roughness,  $\lambda$  is wavelength,  $R_0$  is old target, and  $\theta$  is grazing incident angle. This new target can offset the negative effect of interface roughness.

$$w = \exp(-s^2 \sigma^2 / 2) \quad (1)$$

$$w = \frac{1}{1 + s^2 \sigma^2 / 2} \quad (2)$$

$$R = R_0 \exp[(4\pi \sigma \sin \theta / \lambda)^2] \quad (3)$$

## 2.2. Needle optimization in optilayer software

Traditional optimization method is to optimize thickness distribution of layers in a fixed number of layers by decreasing merit function. While needle optimization is to introduce a material with a small thickness at a boundary or some interior point of a layer. As shown in Fig. 2, there are two materials with refractive index of  $n_H$  and  $n_L$  in a three-layer of two-component coating. A small needle block is introduced into interior point of low-index layer. This special point is determined by calculating  $P(z)$  function by Eq. (4), where  $\lambda$  is wavelength of interest,  $\psi$  is defined by Eq. (5). In Eq. (5),  $n_a$  is refractive index at point  $z_a$ ,  $v$  is weight function,  $R$  is reflectance,  $\hat{R}$  is target reflectance,  $r$  is reflectance coefficient. If  $P(z)$  function deviates zero largely, this point will be selected to introduce a needle block to mitigate this deviation. A merit function change is used to judge whether this needle block is permissible, and to determine the size of needle block. This merit function change is defined by Eq. (6), where  $\hat{n}$  is refractive index of needle block,  $n$  is refractive index distribution, and  $\Delta z$  is the width of needle block. When a needle block at the layer boundary is permissible, the thickness of one component increases, and the thickness of the other component decreases, which is same to traditional optimization method. When a needle block at some interior point of a layer is permissible, the number of layers increases by two. Besides optimizing thickness distribution at fixed dimension, needle optimization also can increase dimension to achieve better spectral performance, which is its

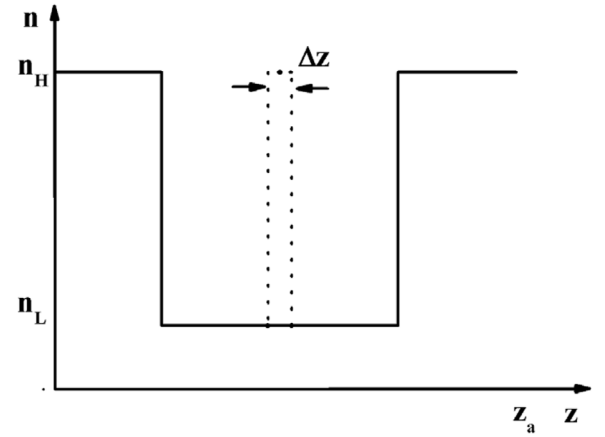


Fig. 2. Needle optimization in Optilayer Software [14].

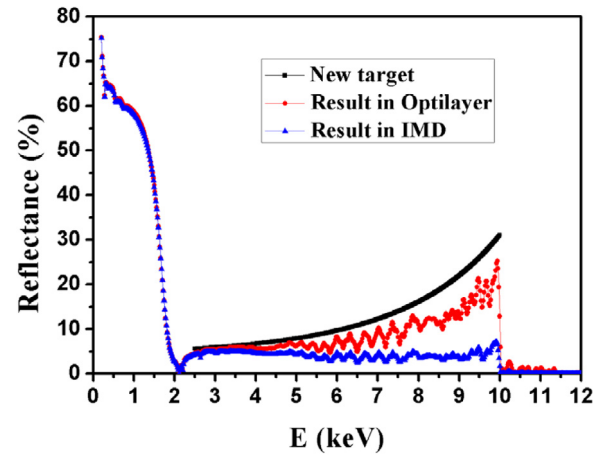


Fig. 3. Design results obtained by Needle optimization at 1.7 degree, and a new target (black line) calculated by Eq. (3) is introduced in Optilayer. (For interpretation of the references to colour in this figure legend, the reader is referred to the web version of this article.)

most distinctive feature. The details about needle optimization can be found in Ref. [14].

$$P(z) = 2\pi \sum_{l=1}^L \frac{1}{\lambda_l} \text{Im} \{ \Psi(z, \lambda_l) \} \quad (4)$$

$$\Psi(z_a, \lambda_l) = \frac{2}{n_a} v_l [R(\lambda_l) - \hat{R}(\lambda_l)] r^*(\lambda_l) [1 + r(\lambda)]^2 \quad (5)$$

$$\delta F = P(\hat{z}) [\hat{n}^2 - n^2(\hat{z})] \Delta z \quad (6)$$

Fig. 3 shows design results obtained by Needle optimization at 1.7 degree, and new target (black line) calculated by Eq. (3) is introduced in Optilayer. Interlayer function is not used in reflectance calculation in Optilayer, but a roughness of 0.45 nm is considered in IMD. The old target is set to be 5%. Thin layer removal is used. Reflectance (red line) increases with increasing of energy in Optilayer, but it (blue line) becomes flat in high energy in IMD due to interface roughness/diffusion effect. The average reflectance is 4% in 5–10 keV.

Fig. 4 shows reflectance curves at 1.0 degree and 1.4 degree obtained by Needle optimization method, and old reflectances are set to be 20% at 1.0 degree, and 10% at 1.4 degree. The average reflectances are 21.2% at 1.0 degree, and 7.4% at 1.4 degree in 5–10 keV.

## 2.3. Refinement in IMD software

Design obtained by Needle optimization can be further optimized by Binda optimization [15] in IMD software. Binda optimization is a

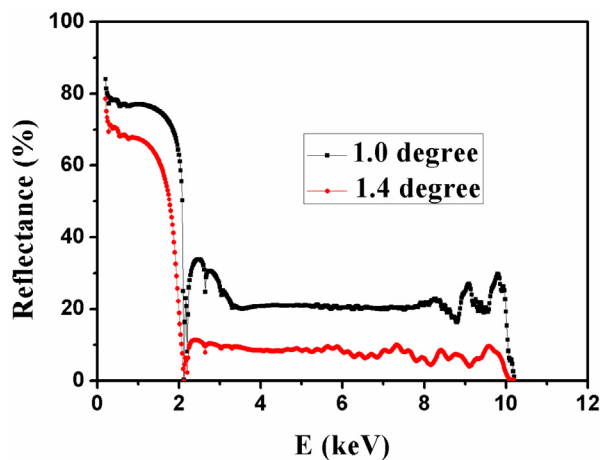


Fig. 4. Reflectance curves at 1.0 degree and 1.4 degree obtained by Needle optimization method.

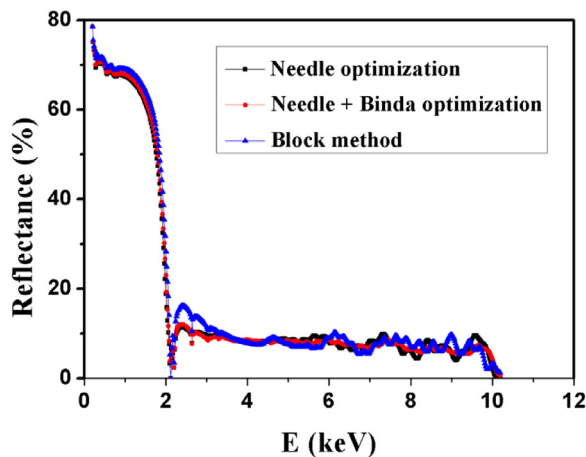


Fig. 5. Design at 1.4 degree further refined optimization by Binda optimization, and comparison of this job with block method. (For interpretation of the references to colour in this figure legend, the reader is referred to the web version of this article.)

kind of genetic algorithm. Compared with traditional genetic algorithm, besides simple reproduction and mutation operators, Binda added more sophisticated mutation and crossover operators in his algorithm. In Binda optimization, one solution for thickness distribution of the supermirror is an individual of population, each individual is modified by replication, mutation, and crossover operators, and better solution is maintained by judging its fitness. This fitness means that the decrease the figure of merit for achieving spectral target. In our refinement by Binda optimization, maximum number is 1000, population size  $P$  is 100 individuals per generation, and fraction of genes that are randomly mutated in each individual  $f_m$  is 20%.

As shown in Fig. 5, a relatively flat curve (blue line) at 1.4 degree is obtained after Binda optimization. For comparison, reflectance curve obtained by block method is also provided. This curve has more oscillations than this job, and 70 layers are used. In our job, only 59 layers are used. The design details about block method can be seen in Ref. [16].

### 3. Conclusion

Interface roughness/diffusion has a great negative influence on reflectance of mirrors in high energy. There is a discrepancy between

Optilayer and IMD softwares when roughness effect is taken into account in designing X ray mirrors by these two softwares. It is found that interlayer function used in Optilayer cannot correctly describe interface roughness effect on reflectance of mirrors, especially in high energy. A modified target is introduced to successfully resolve this problem. Needle optimization shows a slight superiority over block method. Supermirrors working at 1.0, 1.4, and 1.7 degree are successfully designed by Needle optimization.

### CRedit authorship contribution statement

**Xiaodong Wang:** Conceptualization, Methodology, Software. **Hai Tian:** Formal analysis. **Shuai Ren:** Writing - review & editing. **Peng Zhou:** Writing - review & editing. **Bo Chen:** Supervision.

### Declaration of competing interest

The authors declare that they have no known competing financial interests or personal relationships that could have appeared to influence the work reported in this paper.

### Funding

This work was supported by the Joint Research Fund in Astronomy (grant numbers U1731114) under cooperative agreement between the National Natural Science Foundation of China (NSFC) and Chinese Academy of Science (CAS).

### References

- [1] Y. Yao, H. Kunieda, Z. Wang, Design and fabrication of a supermirror with smooth and broad response for hard X-ray telescopes, *Appl. Opt.* 52 (2013) 6824.
- [2] K.D. Joensen, P. Voutov, A. Szentgyorgyi, J. Roil, P. Gorenstein, P. Høghøj, F.E. Christensen, Design of grazing-incidence multilayer supermirrors for hard-x-ray reflectors, *Appl. Opt.* 34 (1995) 7935.
- [3] I.V. Kozhevnikov, I.N. Bukreeva, E. Ziegler, Design of X-ray supermirrors, *Nucl. Instrum. Methods Phys. Res. A* 460 (2001) 424–443.
- [4] A.V. Tikhonravov, M.K. Trubetskov, G. DeBell, Application of the needle optimization technique to the design of optical coatings, *Appl. Opt.* 35 (1996) 5493–5508.
- [5] A.V. Tikhonravov, M.K. Trubetskov, V.V. Protopopov, A.V. Voronov, Application of the needle optimization technique to the design of X-ray mirrors, *Proc. SPIE* 3738 (1999) 248–254.
- [6] A. Tikhonravov, M. Trubetskov, S. Sharapova, Z. Wang, Design of coatings in EUV, soft X-ray and X-ray spectral regions, *Optical Interference Coatings Technical Digest* 2013.
- [7] D.G. Stearns, D.P. Gaines, D.W. Sweeney, E.M. Gullikson, Nonspecular x-ray scattering in a multilayer-coated imaging system, *J. Appl. Phys.* 84 (1998) 1003–1028.
- [8] D.L. Windt, IMD-software for modeling the optical properties of multilayer films, *Comput. Phys.* 12 (1998) 360–370.
- [9] S. Bajt, X-ray focusing with efficient high-NA multilayer laue lenses, *Light Sci. Appl.* 7 (2018) 17162.
- [10] D.D.M. Ferreira, S. Massahi, F.E. Christensen, B. Shortt, M. Bavdaz, M.J. Collon, B. Landgraf, N.C. Gellert, J. Korman, P. Dalampiras, I.F. Rasmussen, I. Kamenidis, M. Krumrey, S. Schreiber, Design, development, and performance of x-ray mirror coatings for the ATHENA mission, *Proc. SPIE* 10399 (2017) 1039918.
- [11] F.E. Christensen, et al., Coatings for the NuSTAR mission, *Proc. SPIE* 8147 (2011) 81470U.
- [12] K. Tamura, et al., Supermirror design for hard X-ray telescopes on-board hitomi (ASTRO-H), *J. Astron. Telesc. Instrum. Syst.* 4 (2018) 011209.
- [13] D.G. Stearns, The scattering of x rays from nonideal multilayer structures, *J. Appl. Phys.* 65 (1989) 491–506.
- [14] Sh. A. Furman, A.V. Tikhonravov, *Basics of Optics of Multilayer Systems*, Edition Frontieres, Gif-sur-Yvette, 1992, p. 242.
- [15] P.D. Binda, F.E. Zocchi, Genetic algorithm optimization of X-ray multilayer coatings, *Proc. SPIE* 5536 (2004) 97.
- [16] X.D. Wang, Design of W/Si supermirror by block method, *Nucl. Instrum. Methods Phys. Res. A* 957 (2020) 163435.